JOURNAL OF VIROLOGY, May 1977, p. 446-458

Vol. 22, No. 2
Printed in U.S.A.

Replication Process of the Parvovirus H-1
IX. Physical Mapping Studies of the H-1 Genome

SOLON L. RHODE III

Putnam Memorial Hospital Institute for Medical Research, Bennington, Vermont 05201

Received for publication 26 November 1976

The cleavage map of H-1 replicative-form DNA to the bacterial restriction endonucleases *Eco*RI, *Hae*II, *Hae*III, *Hin*dII, *Hin*dIII, and *Hpa*II has been determined. The 5'-phosphoryl end of the viral strand is on the right end of the molecule at or near the replication origin. Evidence is presented for the presence of inverted self-complementary sequences at the right end that differ from those at the left end. These sequences allow a foldback of the DNA after denaturation, and a minority of the native replicative-form DNA has the foldback configuration. The possible role of these structures in H-1 DNA synthesis is discussed.

The parvovirus H-1 has a single-stranded DNA genome with a molecular weight of 1.6×10^6. During productive infection, a double-stranded DNA replicative form (RF) is synthesized, and it engages in either a semiconservative replication mode or an asymmetric synthesis of viral progeny DNA (12, 13). Conditional lethal mutants of H-1 have been isolated and were shown to exhibit altered capsid proteins and a temperature-sensitive synthesis of viral progeny DNA (14). Viral RF DNA replication was not temperature sensitive with these mutations.

Analysis by gel electrophoresis and electron microscopy of RF DNA replication using wild-type H-1 and ts1, a mutant temperature-sensitive for progeny DNA synthesis, has shown that the origin for RF DNA replication is near the empirically designated right end of the molecule (15, 17, 18). Replication proceeds by movement of the replication fork within a linear, branched, double-stranded replicative intermediate and terminates at the left end of the molecule. The site-specific cleavage of H-1 RF DNA with the bacterial restriction endonucleases of *Escherichia coli* and *Haemophilus aegyptius*, endo R·*Eco*RI and endo R·*Hae*II, respectively, allowed a partial characterization of the left end of RF DNA (15). It exists as two electrophoretic species of duplex DNA differing in length by about 50 to 70 base pairs (bp), with the smaller form containing some molecules with an alkali-stable linkage of the viral strand (V-strand) to the complementary strand (C-strand). RF DNA molecules exhibited dimerization by base pairing at the left end, and it was proposed that this end of the molecule contains some type of inverted self-complementary sequence (15).

It is the purpose of this study to explore the physical map of H-1 RF DNA in greater detail as a preliminary step to further analysis of the mechanism of H-1 RF DNA replication. The cleavage map of H-1 RF DNA to the restriction endonucleases: *E. coli*, endo R·*Eco*RI; *H. aegyptius*, endo R·*Hae*II and *Hae*III; *H. influenzae*, endo R·*Hin*dII and R·*Hin*dIII; and *H. parainfluenzae*, *Hpa*II; will be described, including its orientation with respect to the viral strand 5'→3' polarity. For simplicity, the restriction endonucleases will be referred to by their abbreviated names. Composite DNA fragments produced by one or more enzymes will be denoted by the algebraic sum of their parts; e.g., *Hin*dII-BA indicates *Hin*dII-B plus *Hin*dII-A or, e.g., *Hae*III-A-*Eco*RI-B indicates the fragment *Hae*III-A minus *Eco*RI-B.

MATERIALS AND METHODS

Virus and cell cultures. For these studies wild-type H-1 was propagated in hamster embryo cultures or NB cells. Virus was titrated by plaque assay in NB cells as described previously (9).

^{32}P-labeled RF DNA. H-1 RF DNA was obtained from NB cell cultures partially synchronized with a single methotrexate block of 16 h. DNA was labeled with [^{32}P]orthophosphate as previously described by incubating infected cultures with medium containing the isotope from 16 to 22 h postinfection at 33°C (15). Viral DNA was extracted and purified through the preparative neutral sucrose gradient step described previously (15). DNA concentrations were determined by the method of Kissane and Robbins (7).

Restriction endonuclease digestion. The restriction endonucleases used here were purchased from Miles Laboratories, Inc., Elkhart, Ind. Digestions were carried out in 10- to 50-μl volumes in the following buffers: (i) endo R·*Eco*RI, 100 mM Tris-hydrochloride (pH 7.5)-50 mM NaCl-10 mM $MgCl_2$-

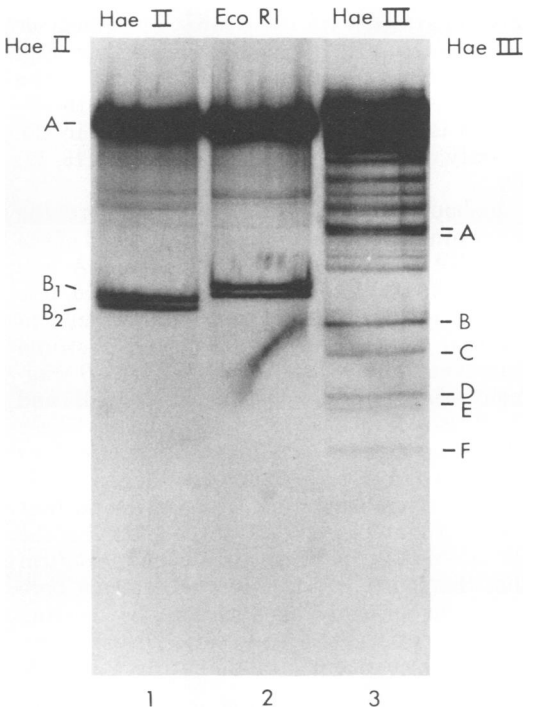

FIG. 1. *Agarose gel electrophoresis pattern of H-1 RF DNA digested by (1) HaeII, (2) EcoRI, and (3) HaeIII (incomplete). Uniformly ^{32}P-labeled H-1 RF DNA was digested by the restriction endonuclease, and the digests were analyzed by electrophoresis in a 1.8% agarose gel for 450 V·h.*

0.1 volume of enzyme diluted 1:10; (ii) *Hae*II, *Hae*III, *Hin*dIII, and *Hpa*II, 6 mM Tris-hydrochloride (pH 7.4)–6 mM 2-mercaptoethanol–6 mM $MgCl_2$–0.05 to 0.1 volume of enzyme; (iii) *Hin*dII, 10 mM Tris-hydrochloride (pH 7.9)–7 mM $MgCl_2$–50 mM NaCl–6 mM 2-mercaptoethanol–0.1 volume of enzyme. For double or sequential digests, incubations were carried out for the enzymes most active in low-ionic-strength buffers first; then NaCl was added to 50 mM, if appropriate, for incubation with the second enzyme.

Reactions were stopped by the addition of 0.5 volume of 2.5% sodium dodecyl sulfate–50% glycerol–1 mM EDTA–20 mM Tris-hydrochloride (pH 7.5), and the samples were analyzed by slab-gel electrophoresis as described previously (15). Fragment sizes were estimated graphically from the plots of log fragment size (in bp) versus mobility (in centimeters of migration). The sizes of marker fragments were estimated by the percentage of total ^{32}P activity present and a molecular weight of 3.26×10^6, or about 4,920 bp for H-1 RF DNA (15). Gels were dried in vacuo and exposed to Kodak Royal X-omat RP/R2 film at room temperature for appropriate times before development.

Isolation of defined fragments. DNA to be isolated for redigestion was located after slab-gel electrophoresis by autoradiography of the wet gel. The gel containing the DNA was excised, diced with a scalpel, and extracted twice for 24 h at 4°C with 10 to 20 volumes of 50 mM Tris-hydrochloride (pH 7.5)–1 mM EDTA. The DNA was concentrated by the addition of 0.1 volume of 3 M sodium acetate (pH 5) and 2.5 volumes of ethanol and precipitation at −20°C for 16 or more h.

Preparation of 5′-$^{32}PO_4$-labeled virion DNA and RF DNA. H-1 virion DNA was prepared from purified virus labeled with [^{3}H]thymidine by alkaline sucrose gradient centrifugation. The DNA was collected by ethanol precipitation after neutralization with HCl and dissolved in 0.1 M Tris-hydrochloride (pH 8.0)–10 mM KCl, and 5 μg of H-1 DNA in 50 μl was treated with 2 μl of *E. coli* alkaline phosphatase (22 U/ml) for 15 min at 65°C (20). The reaction was stopped with the addition of 5 μl of 75 mM EDTA and heated 7 min at 65°C. The following were then added: 10 μl each of 0.01 M $KHPO_4$ (pH 8.0), 1 M KCl, 0.1 M $MgCl_2$ plus 10 mM dithiothreitol, and [γ-^{32}P]ATP (New England Nuclear Corp., Boston, Mass; 30 μCi; specific activity, 1,000 Ci/mmol), 0.5 μl of 500 μM ATP, and finally 3 μl of T4 polynucleotide kinase (3 U/μl) at 0 and 30 min of incubation (10). The reaction was stopped after 60 min at 37°C by the addition of EDTA to 20 mM, and the DNA was fractionated by centrifugation in a 5 to 20% gradient of neutral sucrose in an SW50 rotor for 16 h at 22,500 rpm and 4°C. The viral DNA in the sucrose was mixed with 5 μg of heat-denatured RF DNA in 0.3 ml of 20 mM Tris-hydrochloride (pH 7.4)–0.1 mM EDTA and incubated for 26 h at 65°C. The DNA was precipitated with ethanol overnight and fractionated again by centrifugation in a 5 to 20% neutral sucrose gradient in an SW25 rotor for 22 h at 24,000 rpm and 4°C. The DNA sedimenting in the position of RF DNA at 16*S* was collected, precipitated with ethanol, and redissolved for digestion with restriction endonucleases. The alkaline phosphatase was purchased from Worthington Biochemicals Corp., Freehold, N.J., and T4 polynucleotide kinase was purchased from P-L Biochemicals Inc., Milwaukee, Wis.

RESULTS

Cleavage with endo R·*Eco*RI and endo R·*Hae*II. It was previously shown that *Eco*RI cleaved H-1 RF DNA at a single site in the left half of the molecule, producing the two electrophoretic species of the left end, *Eco*RI-B_1 and -B_2, which comprise about 21% of the total RF DNA (4,920 bp), and the *Eco*RI-A fragment (79% of the total) (15). It was found that *Hae*II also cleaved the RF at a single site estimated here as 60 to 80 bp nearer the left end than *Eco*RI. Figure 1 shows a representative electropherogram of *Eco*RI and *Hae*II digests of RF DNA. Double digestion with *Hae*III and *Eco*RI or *Hae*II revealed that both *Eco*RI and *Hae*II cleaved only the *Hae*III-A fragment (1,570 bp), thus establishing that both cleavage sites are adjacent to the same end of the molecule (data not shown).

Polarity of the RF DNA. The orientation of the V-strand within RF DNA with respect to its 5'-phosphoryl terminus was determined by specifically labeling the 5' terminus of viral DNA with $^{32}PO_4$, using T4 polynucleotide kinase. The labeled viral DNA was separated from the enzymes and fractionated in a gradient of 5 to 20% neutral sucrose. Some of the ^{3}H-labeled viral DNA had fragmented, so the fractions corresponding to full-length viral DNA were pooled and mixed with an equal volume of unlabeled RF DNA (5 μg) in 20 mM Tris (pH 7.5)–0.1 mM EDTA, denatured by heating to 100°C for 10 min immediately before mixing. After a period of annealing, RF DNA was separated from DNA that had not reannealed by a second sedimentation in a gradient of 5 to 20% neutral sucrose, and the RF DNA was precipitated by ethanol. The precipitate was dissolved in 20 mM Tris (pH 7.5)–0.1 mM EDTA after a wash with 70% ETOH–30% 50 mM Tris-hydrochloride (pH 7.5)–1 mM EDTA–0.15 M NaCl to remove traces of Sarkosyl and digested with *Eco*RI or *Hin*dIII and *Eco*RI. The electropherogram in Fig. 2A-2 shows that most of the ^{32}P label migrated with the *Eco*RI-A fragment or with the *Hin*dIII-B fragment (see below; Fig. 2B-3) and is thus at the right terminus of the molecule. Therefore, the 5' terminus of the V-strand is at the right end of RF DNA in the vicinity of the origin for RF replication (15, 17, 18).

It should be noted that a small amount of the 5' terminal label migrated at the left end of the RF DNA as either *Eco*RI-B_1 or *Hae*III-A (see Fig. 7B-2), and this has not been explained. It is not likely that this is the result of random internal locations of 5'-^{32}P-labeled V-strand fragments, since the *Hin*dIII-A–*Eco*RI-B fragment that migrates between *Hin*dII-B and *Eco*RI-B_1 does not appear to be labeled. These data suggest that a small percentage of virions contain DNA strands complementary to the V-strand as previously mentioned (17) and that these account for the 5'-^{32}P at the left end of the RF DNA. An experiment was done to confirm that the source of the C-strand detected here was from virions. This was done by treating purified virions with pancreatic DNase to remove any chance of contaminating C-strands

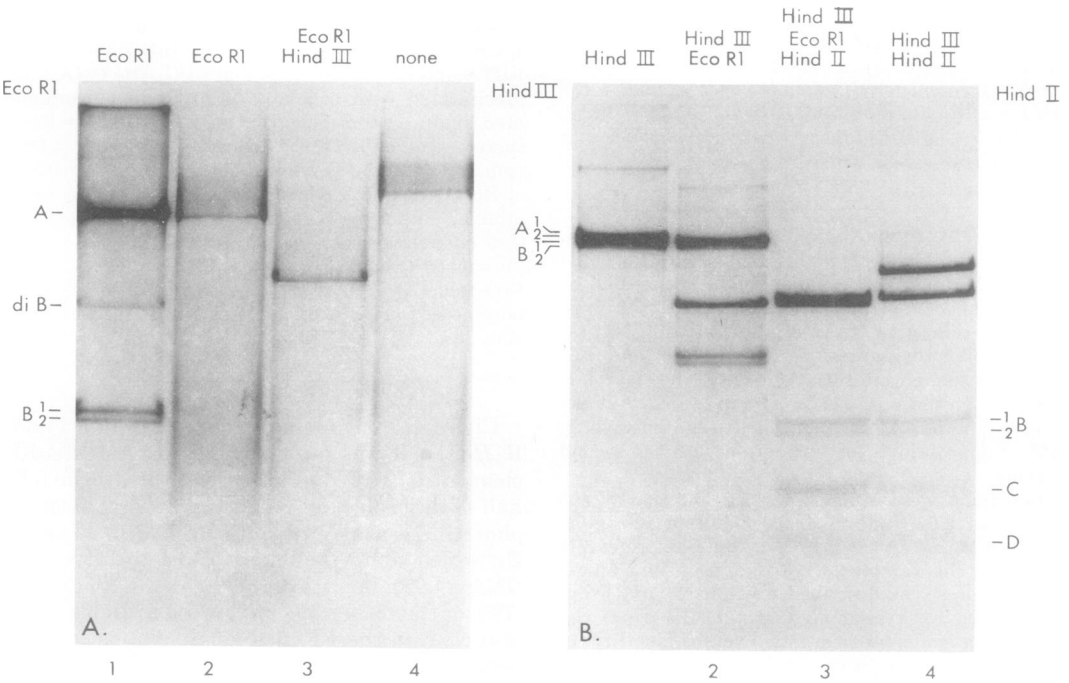

FIG. 2. *(A) Agarose gel electrophoresis pattern of uniformly ^{32}P-labeled H-1 RF DNA (1) or V-strand 5'-$^{32}PO_4$-labeled RF DNA (2 to 4). The DNAs were digested with (1 and 2) EcoRI, (3) EcoRI plus HindIII, or (4) no digestion. Electrophoresis was in a 1.8% agarose gel for 560 V·h. The 5'-^{32}P-labeled band in (3) can be identified as HindIII-B by its mobility relative to EcoRI-B_1 as shown in (B). The four HindIII fragments in (A-1) are visible as separate bands in the original autoradiogram but not in this figure. (B) Agarose gel electrophoresis of uniformly ^{32}P-labeled RF DNA digested with (1) HindIII, (2) HindIII plus EcoRI, (3) HindII plus HindIII plus EcoRI, and (4) HindII plus HindIII. Electrophoresis was in a 1.8% agarose gel for 480 V·h.*

that were not encapsidated. Virion DNA was released from the capsids by heating to 100°C for 3 min in the presence of sodium dodecyl sulfate and annealing the DNA for 2 h at 65°C in 0.3 M NaCl, and the formation of DNA the size of RF DNA was shown by gel electrophoresis (not illustrated). Considering the virion size and density in CsCl, it is most likely that the small proportion of C-strands in the population (about 1 in 400) are encapsidated as single-stranded DNA, but encapsidation of a double-stranded form has not been ruled out.

Cleavage with endo R·*Hin*dII and endo R·*Hin*dIII. Digestion of H-1 RF DNA with *Hin*dIII yields four distinct fragments of nearly equal size and with the mobilities expected for molecules of about half genome length (Fig. 2B-1; the four fragments are distinct on the original autoradiogram, but not in this reproduction). Since the left end is known to have two forms, this result would occur if there is a single cleavage site near the center of the molecule and if the right end also has two different structures. A double digestion with both *Hin*dIII and *Eco*RI demonstrated that the two larger *Hin*dIII fragments, *Hin*dIII-A_1 and -A_2, represent the left half of the molecule (Fig. 2B-2). After digestion with *Eco*RI, the two *Hin*dIII-B fragments are seen to be a major B_1 and a minor B_2, about 100 bp smaller than B_1 (Fig. 2B-2). The minor bands at mobilities less than *Hin*dIII-A are due to incomplete digestion by *Hin*dIII, the cause of which is unknown.

Also shown in this electropherogram are the fragments produced by *Hin*dII and *Hin*dIII with and without an additional digestion with *Eco*RI (Fig. 2B-3 and -4). *Hin*dII cleaves nearer the left end than does *Eco*RI, producing the two left-end fragments *Hin*dII-B_1 and -B_2 of about 645 and 585 bp, respectively, and differing in length by about 60 bp (Fig. 2B-3 and -4 or Fig. 3-4). The large *Hin*dII-A fragment (not present in Fig. 2B) is from the center of the molecule and is cleaved by *Hin*dIII into two fragments of about 1,870 and 1,580 bp, respectively (Fig. 2B-4). The larger of these arises from the left half as it is cleaved by digestion with *Eco*RI (Fig. 2B-3), and together with *Hin*dIII-B they equal *Hin*dIII-A in size (1,870 + 645 = 2,515). By exclusion, the right half contains the *Hin*dII-C (370 bp) and -D (230 bp) fragments; however, the sum of C + D + 1,580 = 2,180, which falls short of *Hin*dIII-B (2,400), suggests the existence of one or more smaller fragments. This was confirmed by electrophoresis of a *Hin*dII digest in a 3% acrylamide-0.5% agarose gel, which revealed that the *Hin*dII-D band resolved into D (230 bp) and E (210 bp). A *Hin*dII-F fragment of about 110 bp was also shown (Fig. 3-4 or 4-1). Also included in this electrophoresis was a *Hin*dII digest of RF DNA labeled at the right end with ^{32}P as described above (Fig. 3-3). The majority of this label at the right end migrated in three bands called E'_1, E'_2, E'_3, which were near *Hin*dII-D or -E in size, but not corresponding to them precisely. Since this molecule was formed by reannealing terminally labeled viral DNA to RF DNA, structures not present in native RF DNA may have been generated. Some 5′ terminal label was present as well in *Hin*dII-F. The terminally labeled fragments did not migrate with *Hin*dII-C or -D. Sequential digestions with *Hae*III and *Hin*dII (Fig. 3-2 and described below) have shown that *Hin*dII-C is cleaved by *Hae*III and that this places *Hin*dII-C to the left of *Hin*dII-D, -E, and -F. Incomplete digests with *Hin*dII yielded major incomplete digestion products of about 800 bp and approximately 450 bp, equivalent in size to CDE and DE, respectively. The position of *Hin*dII-E at the right end was confirmed by sequential digestion with *Hpa*II and *Hin*dII described in a subsequent section. As these fragments, namely, 1,580 + CDE, would complete the size of the right half, the F fragment and minor fragments of about 520 and 300 bp remain to be explained. The minor band of about 520 bp was not present in complete digests, so it can be concluded that it is an incomplete digestion product.

In many electropherograms the E and F fragments were not present in equimolar amounts, and there appeared to be a reciprocal relationship between the amounts of E and F. When a *Hin*dII digest was denatured by heating to 100°C for 3 min and annealed for 22 h at 65°C in 0.5 M NaCl, fragments *Hin*dII-C, -D, and -F were present by electrophoretic analysis, and F was increased in amount. The *Hin*dII-E fragment was absent. The E fragment was found to be stable to heating to 75°C for 10 min at an ionic strength of 0.06 M Na (unpublished data). These findings suggested that *Hin*dII-E may contain self-complementary sequences and that *Hin*dII-F was preferentially generated after heat denaturation. The *Hin*dII-F normally present in digests of unheated DNA may represent the structure present in a minority of the native RF molecules. In fact, the minor form of the right end (*Hin*dIII-B_2), which was about 100 bp smaller, did not produce a minor form of the fragment *Hin*dIII-B–*Hin*dII-CDE (1,480 bp instead of 1,580); therefore, the 100-bp "deletion" must lie in the *Hin*dII-CDE region. The most likely explanation for this is that the minor species of the right end contains *Hin*dII-F,

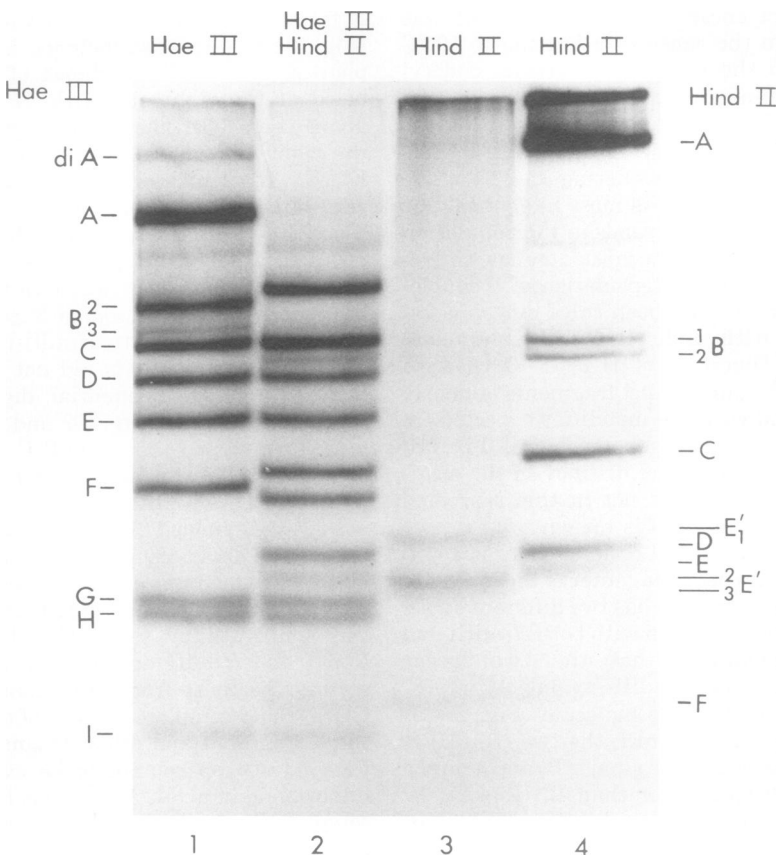

FIG. 3. *Acrylamide gel electrophoresis pattern of uniformly ^{32}P-labeled H-1 RF DNA (1, 2, and 4) or V-strand 5'-$^{32}PO_4$-labeled RF DNA (3). Digestions were by (1) HaeIII, (2) HaeIII plus HindII, or (3 and 4) HindII. Electrophoresis was in a 3% acrylamide-0.5% agarose gel for 540 V·h.*

about 100 bp smaller than *Hin*dII-E. The fragment *Hin*dII-E'$_1$ that was cleaved from DNA produced by hybridization of C-strand DNA to virion DNA prior to digestion was not seen in digests of native RF or in heat-denatured-reannealed *Hin*dII digests. This suggested that reannealing prior to digestion may have been necessary to stabilize the renaturation product that produces *Hin*dII-E'$_1$. These hypotheses were tested by heat denaturing and reannealing RF DNA prior to digestion with *Hin*dII (Fig. 4-3). A fragment with a relative mobility of 0.9 as compared with *Hin*dII-D was produced (arrow), and this is the same relative mobility as *Hin*dII-E'$_1$. When the *Hin*dII digest was heat denatured immediately before electrophoresis, considerable renaturation occurred, but all of the *Hin*dII-E was apparently converted to *Hin*dII-F (Fig. 4-4). The long-term reannealing of a denatured *Hin*dII digest in high salt (Fig. 4-2) was only partially successful in this experiment due to an incomplete digestion.

The origin and location of the *Hin*dII minor band of 300 bp appears to be a 70-bp addition in the *Hin*dII-D region, and it will be called *Hin*dII-D'. This was confirmed by the isolation of a viable defective variant of H-1, containing the *Hin*dII-D' fragment instead of *Hin*dII-D (unpublished data).

In conclusion, the sequence from left to right of the *Hin*dII cleavage fragments is BACDE(F). The *Hin*dII-F fragment appears to be a structural alternative that is present in a minority of native RF molecules. An additional *Hin*dII cleavage site at the extreme right end was discovered with reciprocal digests with *Hpa*II described in the next section.

Cleavage with endo R·*Hpa*II. In preliminary experiments, digests of RF DNA with *Hpa*II were analyzed in 1.4% agarose gels, and no alteration in RF DNA mobility was apparent. To test for cleavage near the ends of the molecule, a sequential digestion with *Hae*III followed by *Hpa*II was analyzed for mobility

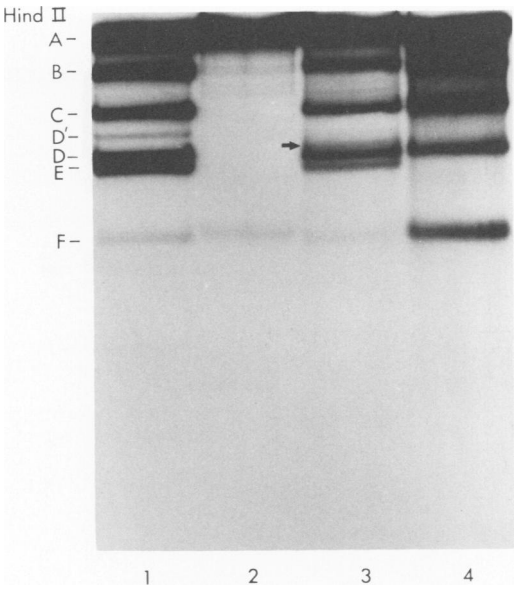

FIG. 4. *Acrylamide gel electrophoresis of uniformly ^{32}P-labeled H-1 RF DNA digested by HindII. The digests were (1) HindII of native RF DNA; (2) HindII digest (incomplete) heated to 100°C for 3 min and incubated for 72 h at 60°C (0.05 M Na^+); (3) RF DNA heated to 100°C for 3 min, incubated for 72 h at 60°C as in (2), and then digested with HindII (the arrow indicates the position of HindII-E'$_L$; and (4) same as (1), but heated to 100°C for 3 min immediately prior to electrophoresis. Electrophoresis was in a 5% acrylamide gel for 400 V·h.*

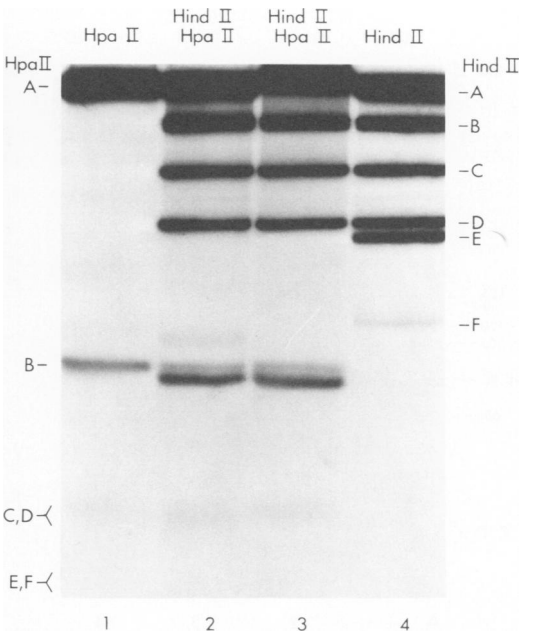

FIG. 5. *Acrylamide gel electrophoresis pattern of uniformly ^{32}P-labeled H-1 RF DNA digested by (1) HpaII, (2) HindII plus HpaII, (3) HindII digest heat denatured (100°C for 3 min to convert HindII-E to HindII-F) and then digested by HpaII, and (4) HindII. Electrophoresis was in a 5% acrylamide gel for 480 V·h.*

shifts of *Hae*III-A or *Hae*III-B, the left and right terminal *Hae*III fragments (see below). The results indicated that *Hpa*II cleaved only *Hae*III-B (not shown). Similarly, a sequential digest with *Hpa*II and *Hin*dII revealed that all of the *Hpa*II cleavage sites were in *Hin*dII-E, the right terminal fragment (Fig. 5-2 and -3).

When *Hpa*II digestions went to completion, the largest of the small *Hpa*II fragments, *Hpa*II-B, migrated at about 80 bp, and diffuse bands were present at about 20 to 30 and 10 to 20 bp (data not shown). In Fig. 6A-1 and -2, incomplete digestions with *Hpa*II are shown, illustrating the products of complete digests and the incompletely digested fragments. The partially digested fragments are at the mobilities of 155, 140, 120, 105, and 60 bp. A similar pattern of incomplete fragments is seen in the *Hin*dII plus *Hpa*II reciprocal digests (Fig. 6B-1), but the *Hpa*II fragments show a slight increase in mobility, which is discussed below.

These findings indicate that *Hpa*II cleaves H-1 RF DNA near the right end, with fragments of about 80, 20 to 30, and 10 to 20 bp. The 80-bp fragment is apparently at the extreme right end, or the *Hin*dII plus *Hpa*II sequential digestions that were incomplete for *Hpa*II (Fig. 6B-1) would have produced a partially digested fragment less than 80 bp smaller than *Hin*dII-E. The incomplete *Hpa*II fragments at 155 and 140 bp suggest that an *Hpa*II fragment of about 15 bp lies on the left end of the collection of small *Hpa*II fragments. Since all partially digested fragments between 80 and 155 bp in size must contain *Hpa*II-B, the incremental differences in their sizes represent the sequential loss of the smaller *Hpa*II fragments. Thus, the fragments are ordered from left to right *Hpa*II-AECFDB, where C and D are the fragments of about 25 bp, and E and F are the fragments of about 15 bp.

An apparent self-contradiction arose when it was observed that in the sequential digestions with *Hin*dII and *Hpa*II, the mobility of *Hpa*II-B and all the incompletely digested *Hpa*II fragments that include *Hpa*II-B had a mobility shift to positions about 5 bp smaller (Fig. 6B-1 and -3). Since these fragments could not be located at the left end of *Hin*dII-E, at 220 bp from the RF DNA right end, another *Hin*dII cleavage site at about 5 bp from the right end must be present. The fact that the 5'-^{32}P terminal label migrated approximately as *Hin*dII-E does not

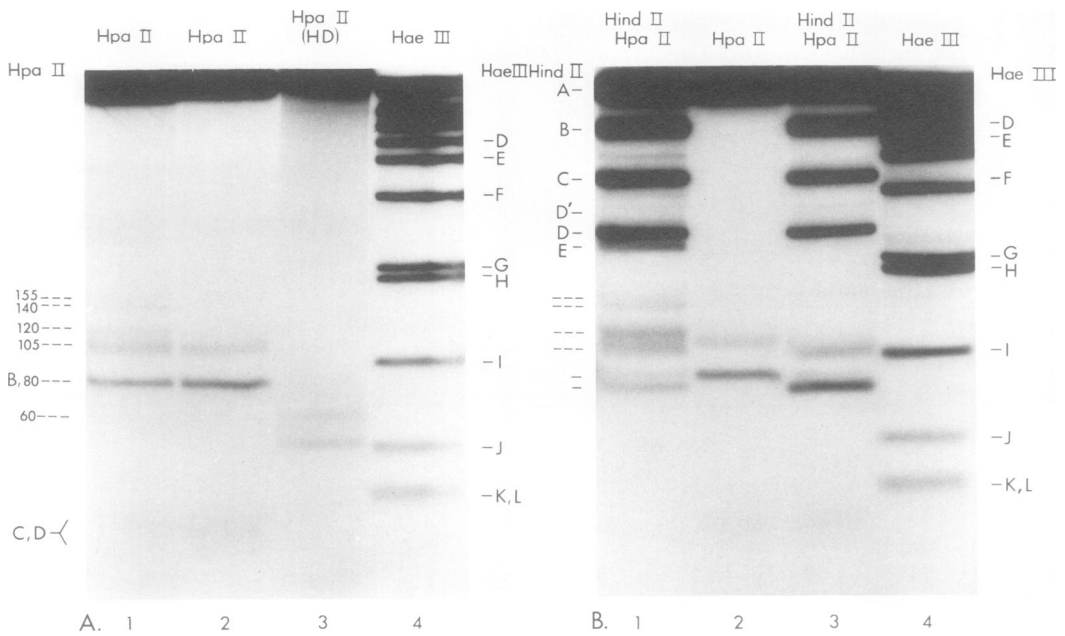

FIG. 6. *(A) Acrylamide gel electrophoresis pattern of uniformly ^{32}P-labeled H-1 RF DNA digested by HpaII or HaeIII. The digests were (1) HpaII (incomplete, 2 h); (2) HpaII (more complete, 14 h); (3) as in (2), heated at 100°C for 3 min prior to electrophoresis; (4) HaeIII. Electrophoresis was in a 5% acrylamide gel for 480 V·h. (B) Acrylamide gel electrophoresis pattern of uniformly ^{32}P-labeled H-1 RF DNA digested by HindII and redigested by HpaII. The digests were (1) HindII and HpaII (incomplete, 3 h); (2) HpaII (incomplete, 5 h); (3) HindII and HpaII [more complete than (1), 12 h], and (4) HaeIII. Electrophoresis was in a 5% acrylamide gel for 480 V·h.*

rule this out, because these molecules had been denatured and apparently do not have the same structure as the native RF DNA. In retrospect, this finding was suggested by a doublet appearance of *Hin*dII-E in incomplete digests, with the faster-migrating fragment becoming predominant as the digestion went to completion (data not shown).

The structure depicted for *Hin*dII-E in Fig. 8 has a number of regions of inverted self-complementary sequences, as manifested by the *Hpa*II and *Hin*dII cleavage sites. These regions would probably cooperate in a foldback renaturation after denaturation to produce *Hin*dII-F. Exactly how this foldback structure is arranged is not clear, since these regions do not appear to have complete symmetry. The digestion of *Hin*dII-F by *Hpa*II as compared with *Hin*dII-E provides some suggestions. The *Hpa*II-B, -E, and -F digestion products appeared to be the same as that from *Hin*dII-E, but *Hpa*II-D was not present and a new fragment appeared with a mobility of a fragment about one-half the size of *Hpa*II-D. Also, *Hpa*II-C appeared to migrate slightly slower than the *Hpa*II-C from *Hin*dII-E (Fig. 6B-2, and -3, not well visualized in reproduction; a similar experiment was also analyzed in a 12% acrylamide gel). Thus, the *Hpa*II cleavage sites bordering *Hpa*II-D appeared to have base paired in the foldback. As these fragments are not well defined under these conditions of electrophoresis (up to 12% acrylamide), this question will require further study.

Cleavage with *Hae*III. Digestion of H-1 RF DNA to completion with *Hae*III yields 12 fragments, A to L, ranging in size from 1,570 to 30 bp (e.g., Fig. 3 and 6B; Table 1). Also noted are several minor bands in the sense that they contain less radioactivity than expected for equimolar amounts of RF and the particular fragment (e.g., Fig. 3 and 7B). These minor fragments, B_1 and B_3, were found adjacent to *Hae*III-B_2, with B_1 having a mobility slower than *Hae*III-B_2, and B_3 migrating ahead of *Hae*III-B_2. They both appear to be in the *Hae*III-B region since they are cleaved by *Hin*dII. It was previously found that *Hae*II and *Eco*RI cleaved *Hae*III-A into their respective B fragments and a fragment representing *Hae*III-A-*Eco*RI-B or *Hae*II-B in size. This result places the *Hae*III-A fragment at the left end. *Hae*III-A has the expected doublet appearance with suitable exposure times, and there is a fragment in limit digests that has a mobility

TABLE 1. *HaeIII fragments of H-1 RF DNA*[a]

*Hae*III fragment	$^{32}PO_4$ content (bp)[b]	Size (bp)[c]
A (includes dimer A)	1,570	1,570
B	810	810
C	650	650
D	480	480-600
E	520	450
F	310	320
G		195
H		180
G + H	375	
I	85	95
J	50	50
K		36
L		34
K + L	70	

[a] The $^{32}PO_4$ content of each *Hae*III fragment was measured by fractionating a complete digest of $^{32}PO_4$-labeled RF DNA by slab-gel electrophoresis in a 3% acrylamide-0.5% agarose gel. The fractions were quantitated by either (i) exposure of the wet gel to X-ray film and excising the gel areas corresponding to each band or (ii) slicing the gel strip into 1.17-mm slices and measuring the ^{32}P by liquid scintillation spectrometry.

[b] The ^{32}P content in each band was converted to a fraction of the total, and the number of bp to the nearest multiple of 5 was calculated by using a total RF DNA size of 4,920 bp (15). The values shown are the averages of six determinations, and the 95% confidence limits were about ±10%.

[c] Sizes of *Hae*III fragments were also determined graphically (log size [bp] versus mobility [centimeters]), using the values in *b*. This allowed estimates of bands G, H, K, and L, which were not completely resolved by the methods for quantitating ^{32}P. It was assumed here that the electrophoretic mobility of cell fragments is only a function of size.

corresponding to a size of *Hae*III-A × 2, which also contains the *Eco*RI or *Hae*II cleavage sites. Since these preparations are known to contain dimer RF molecules linked at the left end, a dimer fragment that includes the left end should be present as in the case of *Eco*RI or *Hae*II (15).

A double digestion of RF DNA with *Hae*III and *Hin*dIII produced a cleavage of *Hae*III-C into C_1, 390 bp, and C_2, 260 bp, thus placing *Hae*III-C at the center of the molecule. The *Hae*III fragments were next grouped into the left or right halves by digesting RF DNA with *Hin*dIII and *Eco*RI and isolating the *Hin*dIII-B and *Hin*dIII-A-*Eco*RI-B fragments. These were digested to completion and analyzed by electrophoresis in a 5% acrylamide gel (Fig. 7A). *Hin*dIII-B as the right half of RF DNA contained *Hae*III-B, -E, -F, -H, -I, -J, -K, and a fragment corresponding to *Hae*III, (*Hin*dIII) C_1. The left half fragment *Hin*dIII-A-*Eco*RI-B yielded on digestion with *Hae*III the following: *Hae*III-D, -G, and -L. *Hae*III-L is apparent as a small fragment of about 30 bp that was unresolved from *Hae*III-K in digests of whole RF DNA. The fragments not corresponding to *Hae*III fragments are *Hae*III-A-*Eco*RI-B and the fragment with the *Hin*dIII cleavage site, *Hae*III (*Hin*dIII) C_2. Thus, the *Hae*III fragments are partially ordered from left to right A (DGL) C_2C_1 (BEFHIJK).

The *Hae*III fragment on the right end of the molecule was determined by digesting the RF DNA labeled at the viral 5'-phosphate as described above (Fig. 7B). Most of the label migrated as *Hae*III-B and appeared to exist as two electrophoretic species. One of these had the mobility of the minor *Hae*III-B_1 fragment, and the major form had a slightly faster mobility than did the major *Hae*III-B_2 fragment. The two *Hae*III-B fragments with the ^{32}P terminal label differed by 40 bp, assuming linear duplex structures in 5% acrylamide, and 20 bp in 3% acrylamide-0.5% agarose and were unresolved in 1.8% agarose. This suggested that one of the B fragments has a nonlinear structure.

Sequential digestion of uniformly labeled RF DNA with *Hae*III and *Hin*dII revealed the expected *Hin*dII cleavage of *Hae*III-A into *Hin*dII-B_1, -B_2, and a fragment of about 900 bp, just larger than *Hae*III-B. *Hin*dII also cleaved the *Hae*III-B and -F fragments (Fig. 3-2). It was also apparent that the *Hin*dII-C fragment had altered mobility, indicating that *Hae*III had cleaved it within about 20 bp of one end. This cleavage must be at the left end of *Hin*dII-C, or the leftward *Hin*dII cleavage site would fall to the left of *Hae*III-F into another *Hae*III fragment, which is contrary to the result obtained. This *Hin*dII cleavage site does reduce *Hae*III-F by about 20 bp and established the linkage *Hae*III-FB, reading from left to right.

Incomplete digests of uniformly labeled RF DNA with *Hae*III produced very complex electropherograms, with more than 50 visible bands, as expected for the various permutations of 11 cleavage sites. Incomplete digests were most useful for determining linkages among the smaller fragments, and these digests were analyzed in gels of 5% acrylamide (data not shown). The small, incompletely digested *Hae*III fragments were of the approximate sizes of 420, 230, 220, and 150 bp. The fragment of 150 bp must consist of some combination of I, J, K, and L, and only fragments JI (50 + 95) would be that size and in the same half of the molecule. Similarly, the fragment at 420 bp consists of IF (95 + 320), since there are no incompletely digested fragments between 420 and 230, a range

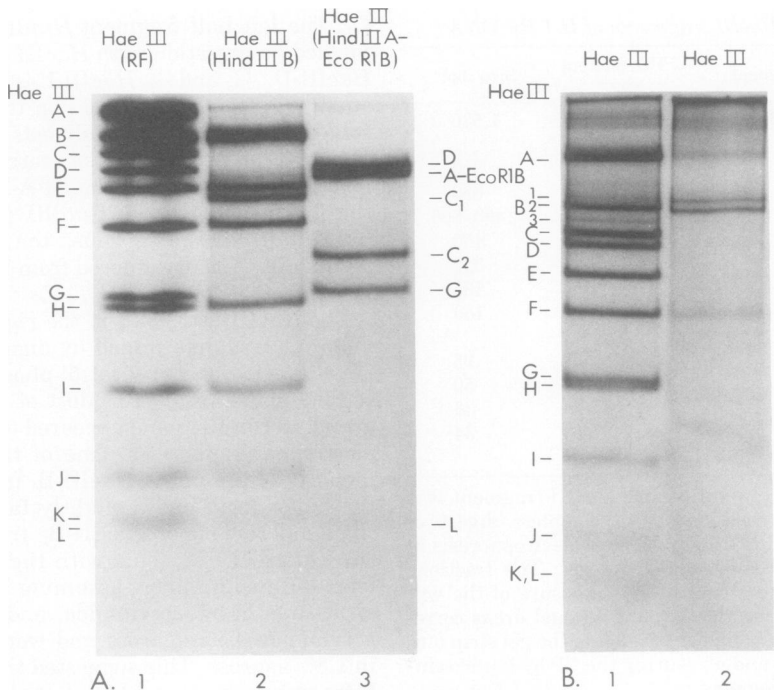

FIG. 7. *(A) Acrylamide gel electrophoresis pattern of HaeIII digests of (1) uniformly ^{32}P-labeled H-1 RF DNA; (2) uniformly ^{32}P-labeled HindIII-B (right half of RF); and (3) HindIII-A-EcoRI-B (left side of RF). HindIII-B and HindIII-A-EcoRI-B were produced by digesting uniformly ^{32}P-labeled RF DNA with HindIII and EcoRI and isolating the fragments by electrophoresis in a 1.8% agarose gel. Electrophoresis was in a 5% acrylamide gel for 480 V·h. (B) Acrylamide gel electrophoresis pattern of HaeIII digests of (1) uniformly ^{32}P-labeled RF DNA and (2) V-strand 5'-$^{32}PO_4$-labeled RF DNA. Electrophoresis was in a 5% acrylamide gel for 520 V·h.*

of 190, so that J, K, and L are excluded. Therefore, the right end is established as JIFB. The fragments of 230 and 220 bp probably consist of LG and HK, respectively, since L and G are in the left half and H and K are in the right half. Analyses of incomplete digests of *Hin*dIII-A-*Eco*RI-B were inconclusive since *Hae*III-A-*Eco*RI-B and *Hae*III-D are both about 500 bp and were not resolved in 1.8% agarose gels. Incompletely digested fragments were present at the mobilities expected for DC_2, DG, and LGD and not present at the mobilities expected for GC_2 or LC_2.

A partial digest of the RF DNA terminally labeled at the right end was made with *Hae*III and analyzed by electrophoresis in a 1.8% agarose gel (electropherogram not shown). The ordered set of fragments in combination with the above data established the complete sequence of *Hae*III fragments. The minor degree of label known to be present in *Hae*III-A at the left end complicated the analysis since it resulted in a detectable band at the positions of *Hae*III-A and bands tentatively identified as AG and RF − B. However, the right-end sequence of IFB was confirmed. The increments in sizes corresponding to J (60 bp) and L (30 bp) were not seen, but the linkages JI and LG were previously established. This experiment was most useful in demonstrating the order AGDCHKEIFB. Thus, the final sequence for *Hae*III is from left to right − ALGDCHKEJIFB.

Fragments with unusual features. In the course of these studies one internal fragment and fragments containing the right end have demonstrated anomalous changes in electrophoretic mobility with changes in gel pore size. Fragments from both areas have shown an apparent increase in molecular weight as gel pore size decreases in comparison with the other fragments that served as the markers. These fragments are *Hae*III-D in the left half and the terminally labeled *Hae*III-B at the right end of the molecule. In Fig. 1, 3, and 7B it is apparent that the relative mobility of *Hae*III-D in comparison with *Hae*III-C or -E is decreasing with the increase in acrylamide concentration. By recovery of ^{32}P, *Hae*III-D has a size of about 480 bp, and in 1.8% agarose it migrates just behind *Hae*III-E at about 480 bp, whereas in 5% acryl-

amide its mobility suggests a size of about 600 bp. This type of behavior in gel electrophoresis has been described for DNA with a more complex structure than the linear duplex (5).

The other fragments that appeared to exhibit electrophoretic characteristics of nonlinear duplexes were the slower-migrating species of the *Hae*III-B fragment of the terminally labeled viral DNA and perhaps the *Hae*III-B_3 fragment of the naturally occurring RF DNA. The former was unresolved from the major *Hae*III-B_2 species in 1.8% agarose gels and migrated as a fragment 40 bp larger, equivalent to *Hae*III-B_1 in 5% acrylamide (e.g., Fig. 7B). The *Hae*III-B_3 fragment was not identified in various 1.8% agarose gels, but migrated at about 710 bp in 3 or 5% acrylamide gels (cf. Fig. 3 or 7B). The exact relationship of structure to the various electrophoretic mobilities of *Hae*III-B is unknown. Cloning of the virus did remove much of the minor *Hae*III-B_1 band, but not *Hae*III-B_3, which is the probable source of the minor fragment *Hin*dII-F as discussed above (Fig. 3-1 versus Fig. 5A-1 or 7B-1). Since *Hin*dII-D′ was also reduced by cloning, it is likely that *Hae*III-B_1 contains *Hin*dII-D′.

A simple hairpin type of inverted self-complementary region would be expected to yield only two, or at most three, structural forms if the "rabbit ear" structure existed in vivo, and only the latter would be nonlinear. The various electrophoretic species of right-end fragments observed in these studies suggest that the structure at the right terminus of H-1 is probably more complex than a simple single palindromic region. The distribution of *Hin*dII or *Hpa*II cleavage sites allows a similar conclusion concerning the complexity of the right terminus as those presented above, except the terminally labeled *Hin*dII fragments did not appear to be nonlinear when their relative mobilities were compared in 3% acrylamide-0.5% agarose versus 5% acrylamide. The terminally labeled *Hin*dII-E_1′ fragment with the slowest mobility did not correspond to a fragment of the natural RF DNA.

DISCUSSION

The physical map of the H-1 genome has been examined by digestion of RF DNA extracted from infected cultures. The cleavage map of H-1 RF DNA to *Eco*RI, *Hae*II, *Hin*dIII, *Hin*dII, *Hae*III, and *Hpa*II is summarized in Fig. 8. A number of interesting structural features of this molecule have become apparent through the electrophoretic behavior of some of the specific fragments generated by the bacterial restriction endonucleases. First, there are the ex-

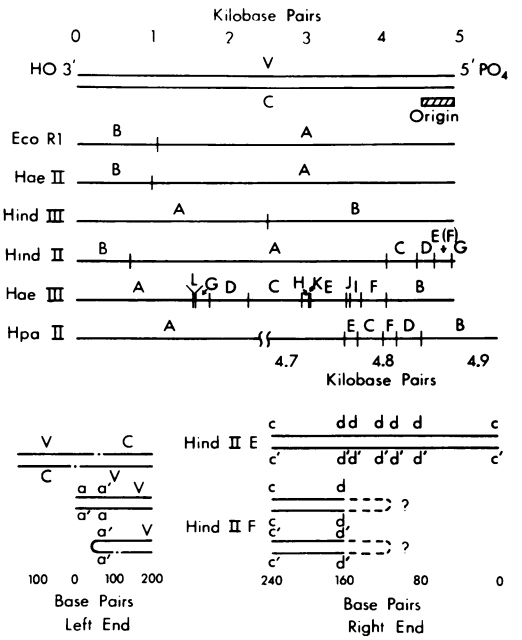

FIG. 8. *Restriction endonuclease cleavage map of H-1 RF DNA. H-1 RF DNA is about 4,920 bp in size (15), and the origin of H-1 RF DNA replication was found to be near the right end (17, 18). The structures proposed for the left and right ends of RF DNA are based on the data in reference 14 and this study. The lowercase letters refer to a base sequence, and their prime indicates its complement. The letters c or c′ are the HindII cleavage sequence, and the letters d or d′ are the HpaII cleavage sequence.*

tended and foldback structural forms of the inverted self-complementary sequence at the left end, a terminus for DNA replication (14, 15, 17, 18). Second, the right end, which is near the origin for RF DNA replication and probably progeny DNA synthesis as well, contains the 5′-phosphoryl terminus of the viral strand (15, 17, 18). This implies that progeny viral DNA synthesis is executed by displacement of a preexisting viral strand in RF DNA by a nascent viral strand being synthesized in a 5′ to 3′ direction. The right end of RF DNA also appears to contain inverted self-complementary sequences, but unlike the left end no evidence of a covalent linkage of V-strand to C-strand at the right end has been obtained. Since virion DNA has not been observed to circularize or dimerize and the left end does not contain *Hin*dII or *Hpa*II cleavage sites, it is unlikely that the right and left ends contain the same sequences such as those described for adenovirus-associated virus (AAV) (1, 18). This observation may be directly relevant to the fact that H-1 progeny DNA synthesis and RF DNA repli-

cation are highly polar and exhibit a unique origin and terminus. The presence of equal portions of both + and − strands in AAV virions implies that the origin for AAV progeny DNA synthesis may occur at either end of an AAV RF DNA.

It should be remarked that the structures proposed for the right terminus in Fig. 8 are based on the positions of the *Hin*dII and *Hpa*II cleavage sites, but they may be too simplistic and more information on the base sequences in this region will be needed to predict the structure of the two *Hin*dII-F foldbacks in the V- and C-strands. The data described here imply an odd number of *Hpa*II cleavage sites and suggest the presence of asymmetry in the foldback structures. Such asymmetries would make it possible for virion proteins to recognize (bind) specifically the foldback structure of the V-strand and thus effect an asymmetric synthesis of progeny viral DNA, but only if the foldback is not transferred from one strand to the other. If an asymmetric foldback is transferred from the C-strand to the V-strand, then its polarity is reversed and it can no longer be a V-strand-specific terminus. Consequently, two types of foldback regions could occur in V-strand DNA with either the nonpalindromic sequences of the parental virion or an inversion of their complement. A more detailed study of the physical map of this region should determine whether the right end of RF DNA or the foldback region at the 5′ terminus of virion DNA is unique or includes the inverted complement as well. The structure emerging for herpes simplex DNA has very interesting features concerning this problem (4, 21, 22). It appears that the unique structural gene sequences are divided into two parts, which are located in the turnaround areas of two foldback sequences rather than in the body of the molecule. The most relevant observation is that the unique sequences appear to occur in various permutations with respect to their polarity, which is the predicted consequence of the Cavalier-Smith replication model (2). Thus, herpes simplex DNA may be a molecule consisting of two large foldback ends and no middle, with the structural genes lying in the nonpalindromic regions of the turnarounds.

With the naturally occurring RF DNA uniformly labeled and extracted from infected cells, there were three types of *Hae*III-B fragments, B_1, B_2, and B_3. The terminally labeled hybridization product exhibited four *Hin*dII right-end fragments, three of which did not correspond to those of the natural RF DNA. One of these, the slower-migrating species of terminally labeled fragment, was shown to arise by *Hin*dII digestion of reannealed RF DNA, but not on reannealing of *Hin*dII fragments. It did not exhibit the electrophoretic behavior of nonlinear DNA expected from the observed changes in mobility of the *Hae*III-B fragments. This may be the result of the loss of a large portion of the linear duplex "stem" portion of the *Hae*III-B DNA. The *Hin*dII-E fragment was converted to *Hin*dII-F apparently by unimolecular hybridization of one or more inverted self-complementary region(s) at the right terminus. This region appears to be about 105 to 120 bp in length. The cluster of *Hpa*II cleavage sites, which contain the sequence of 5′ C C G G 3′ (6), is in a region previously deduced to be G-C rich by virtue of its high melting temperature (18).

The significance of the apparent nonlinear structure of the internal *Hae*III-D fragment as inferred by its electrophoretic behavior is unknown. As this region is not near the origin for DNA replication, it is probably not directly concerned with that process. A more likely possibility is a role in regulation of transcription, since the location of the D fragment could be a region that contains an origin for synthesis of of mRNA for virion protein. Inverted self-complementary regions in fd DNA have been located in the vicinity of promotor regions for fd mRNA synthesis (16). The transcriptional mapping studies of the H-1 genome in progress should help validate this possibility.

Finally, the variant RF DNA species that contains an addition in the *Hin*dII-D region is of special interest. Additions that consist of reiterations of the origin for DNA replication have been described for other viruses (e.g., reference 3), and the location of *Hin*dII-D is compatible with our previous estimations of the location of the origin for RF DNA replication (17, 18). Experiments are in progress to determine whether the replication origin is internal in the *Hin*dII-D fragment or closer to the right end in *Hin*dII-E.

The existence of the inverted self-complementary sequences implied by these and preceding studies at the ends of the linear H-1 RF DNA supports the model for replication of eukaryotic chromosome ends proposed by Cavalier-Smith (2). The essential feature of this model is the transfer of an inverted self-complementary foldback region (palindrome) from one strand to its complement, thereby supplying a presynthesized 5′-phosphoryl terminus and both the template and 3′-OH primer for completion of the 3′-OH terminus of the chromosomal end. This model implicates the existence of a

site-specific endonucleasae that makes the cleavage releasing the foldback region from its parent strand. This cleavage would occur only after ligation of the foldback region to the C-strand or after it has served its function as primer for initiation of C-strand synthesis; otherwise, the foldback region would be released from the molecule. If the foldback region serves as a primer, it follows that, during progeny DNA synthesis in the presence of a radiolabeled substrate, the first initiation would produce an unlabeled virion DNA, the second would produce a virion DNA labeled in all regions except the foldback at the origin, and not until the third initiation would a fully labeled virion DNA be released. In the case of RF DNA replication a similar combination of old and new DNA would occur as previously discussed (2). Another possible mechanism of replication would utilize the terminal palindrome to establish a transient covalent linkage between DNA strands, which would allow an RNA-primed nascent strand to bridge from one strand to its complement, after which the site-specific endonuclease would nick the foldback, returning it to its original strand. In this case old and new DNA would not be linked. Other variations on this scheme are also possible. During the preparation of this manuscript, a modification of the Cavalier-Smith model, a rolling hairpin model, which assumes that the origin for DNA replication is self-primed at a palindromic terminus, was proposed for the parvovirus MVM (minute virus of mice) DNA synthesis (19). The experimental data cited by these authors concerning self-complementary sequences at the termini of MVM virion DNA are in agreement with our results with H-1 (15). The model proposed for MVM DNA replication is not compatible in many respects with our data for H-1: (i) H-1 progeny DNA synthesis appeared to occur in RF DNA monomers and not necessarily in concatamers (8, 12, 13); (ii) the synthesis of the majority of dimer molecules of ts1 at the restrictive temperature was not by a rolling hairpin mechanism or nondisjunction of daughter molecules of a replicating monomer RF DNA (15); (iii) concatamers greater than 2 N were absent or present in very low concentrations (15); (iv) the covalent linkages of the V- to C-strand were not at the origin but predominantly, if not entirely, at the left end of RF DNA, a terminus for DNA replication; (v) this model does not account for monomer RF DNA replication with branched double-stranded replicative intermediates (17, 18) from which progeny DNA synthesis may be a simple specialization modulated by virion protein.

The fortuitous cleavage by *Hpa*II and *Hin*dII within the foldback region at the right terminus of RF DNA and presumably virion DNA will allow a convenient experimental attack on the problem of whether the foldback region is transferred from one strand to the other as hypothesized by Cavalier-Smith (2).

ACKNOWLEDGMENTS

This research was supported by Public Health Service grant CA-07826-11 from the National Cancer Institute.

I gratefully acknowledge Jessica Bratton for expert technical assistance, Rob Costantino for illustrations, and Virginia Haas and Janeen Pratt for secretarial duties.

LITERATURE CITED

1. **Berns, K. I., and T. J. Kelley, Jr.** 1972. Visualization of the inverted terminal repetition in adeno-associated virus DNA. J. Mol. Biol. 82:267-271.
2. **Cavalier-Smith, T.** 1974. Palindromic base sequences and replication of eukaryote chromosome ends. Nature (London) 250:467-470.
3. **Davoli, D., and G. C. Fareed.** 1974. Amplification of a circular segment of SV40 DNA. Nature (London) 251:153-155.
4. **Delius, H., and J. B. Clements.** 1976. A partial denaturation map of herpes simplex virus type 1 DNA: evidence for inversions of the unique DNA regions. J. Gen. Virol. 33:125-133.
5. **Dingman, C. W., M. P. Fisher, and T. Kakefuda.** 1972. Role of molecular conformation in determining the electrophoretic properties of polynucleotides in agarose-acrylamide gels. Biochemistry 11:1242-1250.
6. **Garfin, D. E., and H. M. Goodman.** 1974. Nucleotide sequences at the cleavage site of two restriction endonucleases from *Hemophilus parainfluenzae*. Biochem. Biophys. Res. Commun. 59:108-116.
7. **Kissane, J. M., and E. Robbins.** 1958. The fluorometric measurement of deoxyribonucleic acid in animal tissues with special reference to the central nervous system. J. Biol. Chem. 223:184-188.
8. **Kongsvik, J., J. Gierthy, and S. L. Rhode.** 1974. Replication process of the parvovirus H-1. IV. H-1-specific proteins synthesized in synchronized human NB kidney cells. J. Virol. 14:1600-1603.
9. **Ledinko, N.** 1967. Plaque assay of the effects of cytosine arabinoside and 5-iodo-2'-deoxyuridine on the synthesis of H-1 virus particles. Nature (London) 214:1346-1347.
10. **Lillehaug, J. R., and K. Kleppe.** 1975. Effect of salts and polyamines on T4 polynucleotide kinase. Biochemistry 14:1225-1229.
11. **Rhode, S. L.** 1973. Replication process of the parvovirus H-1. I. Kinetics in a parasynchronous cell system. J. Virol. 11:856-861.
12. **Rhode, S. L.** 1974. Replication process of the parvovirus H-1. II. Isolation and characterization of H-1 replicative form DNA. J. Virol. 13:400-410.
13. **Rhode, S. L.** 1974. Replication process of the parvovirus H-1. III. Factors affecting H-1 RF DNA synthesis. J. Virol. 14:791-801.
14. **Rhode, S. L.** 1976. Replication process of the parvovirus H-1. V. Isolation and characterization of temperature-sensitive H-1 mutants defective in progeny DNA synthesis. J. Virol. 17:659-667.
15. **Rhode, S. L.** 1977. Replication process of the parvovirus H-1. VI. Characterization of a replication terminus of H-1 replicative-form DNA. J. Virol. 21:694-712.
16. **Shen, C.-K. J., and J. E. Hearst.** 1976. Psoralen-cross-linked secondary structure map of single-stranded

virus DNA. Proc. Natl. Acad. Sci. U.S.A. 73:2649-2653.
17. **Singer, I. I., and S. L. Rhode.** 1977. Replication process of the parvovirus H-1. VII. Electron microscopy of replicative-form DNA synthesis. J. Virol. 21:713-723.
18. **Singer, I. I., and S. L. Rhode.** 1977. Replication process of the parvovirus H-1. VIII. Partial denaturation mapping and localization of the replication origin of H-1 replicative-form DNA with electron microscopy. J. Virol. 21:724-731.
19. **Tattersall, P., and D. C. Ward.** 1976. Rolling hairpin model for replication of parvovirus and linear chromosomal DNA. Nature (London) 263:106-109.
20. **Weiss, B., T. R. Live, and C. C. Richardson.** 1968. Enzymatic breakage and joining of deoxyribonucleic acid. J. Biol. Chem. 243:4530-4542.
21. **Wilkie, N. M.** 1976. Physical maps for herpes simplex virus type 1 DNA for restriction endonucleases *Hin*dIII, *Hpa*-1, and *X. bad*. J. Virol. 20:222-233.
22. **Wilkie, N. M., and R. Cortini.** 1976. Sequence arrangement in herpes simplex virus type 1 DNA: identification of terminal fragments in restriction endonuclease digests and evidence for inversion in redundant and unique sequences. J. Virol. 20:211-221.